

New Pyrrole-Based Organic Dyes for Dye-Sensitized Solar Cells: Convenient Syntheses and High Efficiency

Qianqian Li, Lanlan Lu, Cheng Zhong, Jing Huang, Qing Huang, Jie Shi, Xianbo Jin, Tianyou Peng,* Jingui Qin,* and Zhen Li*^[a]

As petroleum and coal are depleted, renewable energy sources have attracted increasing attention in recent years, and solar energy is considered as a good alternate for fossil fuel energy. Due to the advantages of low cost, easy production, flexibility, and transparency relative to conventional crystalline silicon solar cells, dye-sensitized solar cells (DSSCs) have emerged as an important class of photovoltaic devices, since the breakthrough was made by Grätzel and co-workers.^[1] Thanks to the enthusiastic efforts of scientists, significant progress was made in terms of the performance of DSSC devices: power conversion efficiencies above 11% in standard global air mass (AM) 1.5 have been achieved by several Ru^{II}-polypyridyl complexes,^[2] while 6–9% was shown by metal-free organic dyes.^[3] Although the efficiency of the latter was a little lower, they possessed some advantages over the former: ease of synthesis, high molar extinction coefficient, tunable absorption spectral response from the visible to the near infrared (NIR) region, as well as environmentally friendly and inexpensive production techniques. To further improve the efficiencies of pure organic-dye-based DSSCs, the structure and physical properties of the sensitizer are clearly important, especially the conjugation across the donor and anchoring groups, and good electronic coupling between the lowest unoccupied orbital (LUMO) of the dye and the conduction band of TiO₂, which is very important for high electron-transfer rates.^[4] Thus, in order to exploit such sensitizers, it is necessary to lower the energy of the charge-transfer transition. In this respect, some electron-rich heteroaromatic rings have been used as bridges between

electron donor and acceptor: some thiophene and furan-containing dyes exhibited good device efficiencies,^[5] due to their smaller resonance energy in comparison with that of benzene (thiophene, 29; furan, 16; benzene, 36 kcal mol⁻¹). However, the analogue of furan and thiophene moieties, that is pyrrole group, has seldom been used as a conjugated bridge in organic dyes,^[6] possibly due to its instability, although it possesses a smaller resonance energy (21 kcal mol⁻¹), and could be easily functionalized, not only on the *ortho*-position to the nitrogen atom, but also through the substituted reactions on the N–H bond.^[7] Fortunately, our recent research and some reports of other groups demonstrated that its stability could be enhanced dramatically by inserting it into a π system and substituting the H atom on the N atom. Some exciting results have been obtained from pyrrole-containing materials in several different research fields (including photochemistry,^[8] second-order nonlinear optical chromophores,^[9] and two-photon absorption materials^[10]).

On the other hand, the aggregation of the dyes on the semiconductor surface would sharply decrease the power conversion efficiency of DSSC, as a result of the influenced light absorption caused by the filtering effect.^[11] Thus, to achieve optimal performance, possible aggregation should be avoided through appropriate structural modification. According to our experience in the research of aggregation-induced emission (AIE) materials, the introduction of non-coplanar aromatic rings through single bonds helps to avoid of the aggregation.^[12]

Therefore, taking all the above-mentioned points into consideration, we designed two new pyrrole-containing dyes, LI-1 and LI-2, in which the triphenylamine (TPA) group was used as the electron donor and a cyanoacrylic acid moiety as the anchoring group. Another TPA group in LI-1 was linked to the pyrrole ring through the carbon–nitrogen single bond to suppress the aggregation of the dye on the surface of TiO₂. For comparison, a carbazolyl (Cz) group with more planar structure was used instead of TPA in LI-2. These two dyes were conveniently obtained, and demon-

[a] Q. Li, L. Lu, C. Zhong, J. Huang, Q. Huang, J. Shi, Prof. X. Jin, Prof. T. Peng, Prof. J. Qin, Prof. Z. Li
Department of Chemistry,
Wuhan University, Wuhan 430072 (P.R. China)
Fax: (+86)27-68756757
E-mail: lizhen@whu.edu.cn
typeng@whu.edu.cn
jgqin@whu.edu.cn

Supporting information for this article is available on the WWW under <http://dx.doi.org/10.1002/chem.200901150>.

Table 1. Some characterization data of LI-1 and LI-2.

	$\lambda_{\max}^{[a]}$ [nm]	$\lambda_{\max}^{[b]}$ [nm]	$E_{0,0}^{[c]}$ [eV]	$E_p^{[d]}$ [V]	$E_{\text{ox}}^{[e]}$ [V] vs. NHE	$E_{\text{red}}^{[f]}$ [V] vs. NHE	$E_{\text{gap}}^{[g]}$ [V]
LI-1	448	449	2.34	0.86, 1.01	1.06	-1.28	0.78
LI-2	415	431	2.40	0.60, 0.82	0.80	-1.60	1.10

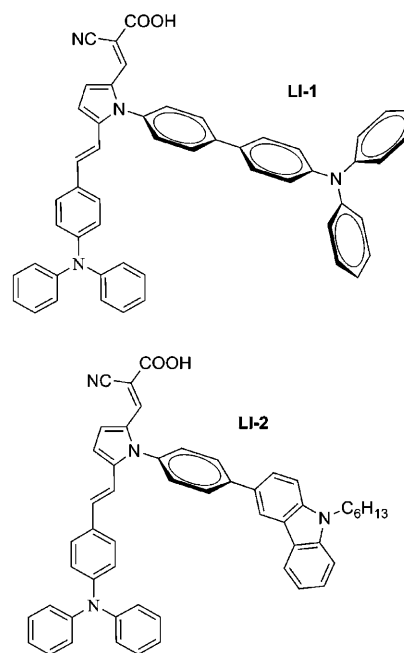
[a] Absorption spectra of dyes measured in ethanol with the concentration of 3×10^{-5} M. [b] Absorption spectra of dyes adsorbed on the surface of TiO_2 . [c] The bandgap, $E_{0,0}$ was derived from the observed optical edge. [d] E_p is the peak of DPV (the DPV of the dyes were measured in CH_2Cl_2 with 0.1 M $(n\text{-C}_4\text{H}_9)_4\text{NPF}_6$ as electrolyte (scanning rate, 100 mV s^{-1} working electrode and counter electrode, Pt wires; reference electrode, Ag/AgCl)). [e] The oxidation potential (E_{ox}) referenced to calibrated Ag/AgCl was converted to the NHE reference scale: $E_{\text{ox}} = E_p + 0.197 \text{ V}$. [f] E_{red} was calculated from $E_{\text{ox}} - E_{0,0}$. [g] E_{gap} is the energy gap between the E_{red} of dye and the CB level of TiO_2 (-0.5 V vs. NHE).

strated high conversion efficiencies (up to 91% of the standard cell from N719). Herein, we report their syntheses, structural characterization, electrochemical properties, theoretical calculations, and photovoltaic performance.

The whole synthetic route is shown in Scheme S1 along with the detailed preparation procedure is described in the Supporting Information. 4-Bromophenylpyrrole (**1**), the important spacer between the electron donor and the electron acceptor, was synthesized from 2,5-dimethoxy tetrahydrofuran and 4-bromoaniline with high yield,^[13] then 4-bromophenylpyrrole-2-carbaldehyde (**2**) was obtained through normal Vilsmeier reaction. Compound **2** was treated with **3** under Wittig–Hornor reaction conditions to yield compound **4**. Another Vilsmeier reaction led to the introduction of an aldehyde group to the pyrrole ring, and was followed by a Suzuki reaction with triphenylamine and carbazole-based boronic acid to give compounds **6** and **7**, respectively. Finally, the two dyes were obtained through a Knoevenagel condensation reaction of **6** or **7** with cyanoacetic acid in the presence of piperidine.

The reaction products were characterized by spectroscopic analyses, and all give satisfactory data (some data listed in Table 1) corresponding to their expected molecular structures (see Supporting Information for details). As shown in their IR spectra (Figure S1), the strong peak of the cyanide groups in the two dyes were observed at about 2217 cm^{-1} , indicating the success of Knoevenagel condensation reaction between **6** or **7** and cyanoacetic acid. The absence of the peak derived from the aldehyde groups at about $\delta = 10.0 \text{ ppm}$ in their $^1\text{H NMR}$ spectra further confirmed the complete conversion of the aldehyde groups to cyanoacrylic acid moieties as the anchoring groups. LI-1 and LI-2 (see below) are thermally stable, and their initial decomposition temperatures were found to be 248 and 283 °C, respectively, by thermal gravimetric analysis (TGA) under argon.

The two dyes are soluble in common organic solvents, such as dichloromethane, THF, DMF, and DMSO. As shown in their UV/Vis spectra tested in ethanol (Figure S2 in the Supporting Information, Table 1), LI-1 and LI-2 give two distinct absorption bands: a solvent-independent band at $\lambda_{\max} < 400 \text{ nm}$ derived from the localized $\pi\text{-}\pi^*$ transition and another solvent-dependent band at λ_{\max} in the range of 400–600 nm, which could be ascribed to an efficient charge-separated state produced by an intramolecular charge transfer (ICT) between the donor and the cyanoacrylic acid anchoring moiety. In addition, the charge-transfer bands exhibit a negative solvatochromism, that is, blue shift in more polar



solvents (Table S1 and Figures S3, S4, and S5 in the Supporting Information). This could be attributed to the deprotonation of the carboxylic acid, which decreases the pulling ability of the electron acceptor. Similar phenomena have been reported in the case of black dye and other metal-free organic dyes.^[2,14] LI-1 shows much higher extinction coefficients ($\epsilon = 40\,500 \text{ M}^{-1} \text{ cm}^{-1}$) than that of LI-2 ($\epsilon = 27\,900 \text{ M}^{-1} \text{ cm}^{-1}$), both of which is higher than that of Ru–organic complex N719 ($\epsilon = 14\,100 \text{ M}^{-1} \text{ cm}^{-1}$ in ethanol), indicating that they are beneficial to light harvesting. After being adsorbed on the surface of TiO_2 , the maximum absorption wavelengths do not show a big difference as compared to those in ethanol (Figure S6 in the Supporting Information). However, the absorption threshold is red-shifted by about 60–80 nm, owing to the increased delocalization of the π^* orbital of the conjugated framework caused by the interaction between the carboxylate group and the Ti^{4+} ions, which directly decreases the energy of the π^* level. The amounts of the adsorbed dye on the TiO_2 films were estimated by desorbing the dye with basic solution; the surface concentrations were determined to be 1.08×10^{-7} and 1.40×10^{-7} for LI-1 and LI-2, respectively.

To investigate the possibility of electron transfer from the excited dye molecule to the conductive band of TiO_2 and

also dye regeneration, the electrochemical characteristics of the dyes were investigated by using differential pulse voltammetric (DPV) methods (Figure S7 in the Supporting Information and Table 1). The oxidation potential of the dyes was determined from the peak potentials (E_p) by DPV; the oxidation potential versus NHE (E_{ox}) corresponds to the highest occupied molecular orbital (HOMO), while the reduction potential versus NHE (E_{red}), which corresponds to the lowest unoccupied molecular orbital (LUMO), can be calculated from $E_{ox} - E_{0,0}$. As shown in Figure 1, both the

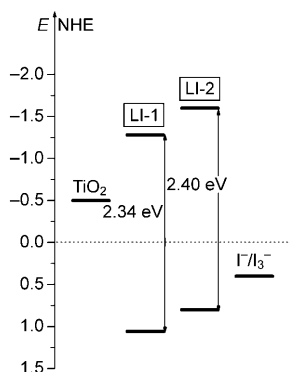


Figure 1. Schematic representation of the band positions in DSSCs based on LI-1 and LI-2. The energy scale is indicated in electron volts using the normal hydrogen electrode (NHE).

LUMO and HOMO levels of these dyes agree with the requirement for an efficient sensitizer: First, their LUMO levels are below the conductive band (CB) level (-0.5 V vs. NHE) of TiO₂, and the E_{gap} values range from 0.78–1.10 V, which are all larger than the gap from N719 ($E_{gap} = 0.35$ V). Assuming that energy gap of 0.2 eV is necessary for the efficient electron injection, these driving forces are large enough for the injection; secondly, the HOMO levels of the dyes are more positive than the iodine redox potential (0.4 V). Thus, these oxidized dyes can be regenerated from the reduced species in the electrolyte to give an efficient charge separation and can be used as sensitizers that should function well, since the electron transfer in DSSCs is feasible.

To get an insight into the molecular structure and electron distribution of the organic dyes, the geometries of LI-1 and LI-2 were optimized by using time-dependent DFT (TDDFT) calculations with the Gaussian 03 program.^[14c] In particular, we used the B3LYP exchange-correlation functional and a 6-31 g* basis set; solvation effects were included by means of the polarizable continuum model. To model the electronic state of the dyes adsorbed on the TiO₂ surface, we employed the dye's potassium salt, since the dye should be bonded to the TiO₂ surface in its carboxylate form. The electron distribution of the HOMOs and LUMOs are shown in Figure 2. It reveals that the dyes are completely planar except for the triphenylamine and carbazole moieties, which are linked with pyrrole through a single carbon–nitrogen bond to avoid sterical clashes. In addition the triphenyl-

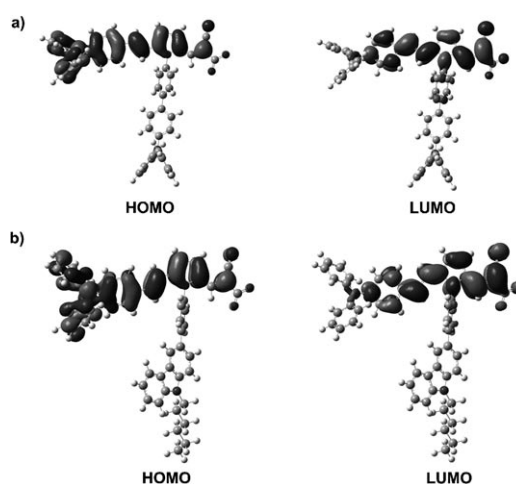


Figure 2. Frontier orbitals of the dyes a) LI-1 and b) LI-2 optimized at the B3LYP/6-31+G (D) level.

amine group exhibits a more bulky three-dimensional structure. The theoretical results give two or three transitions with large oscillator strengths (f) for the dyes that are consistent with the absorption spectra. A HOMO→LUMO transition is centered in the visible light field with large oscillator strengths $f = 1.0$ – 1.3 and a combined transition for a band in the UV region ascribed to HOMO–2→LUMO, HOMO–1→LUMO, and HOMO→LUMO+2 transitions with a lower f value (Table S2 in the Supporting Information). It should also be noted that the HOMO→LUMO excitation induced by light irradiation could move the electron distribution from the dyes to the anchoring moieties. Assuming similar molecular orbital geometry when anchored to TiO₂, the position of the LUMO close to the anchoring groups would surely enhance the orbital overlap with the titanium 3d orbitals and thus benefit the electron injection from dyes to TiO₂.^[15]

Figure 3 shows the current-density/voltage characteristics of the DSSCs obtained with the two sensitizers based on pyrrole, and the detailed photovoltaic performance param-

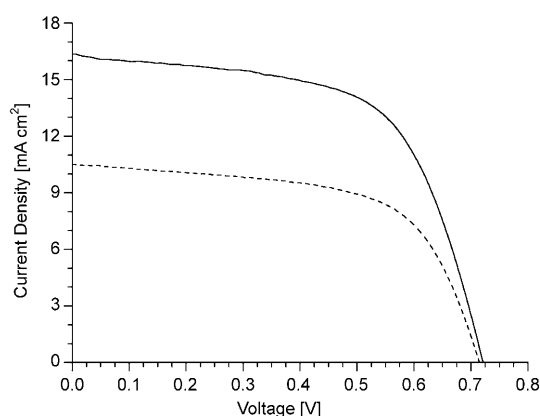


Figure 3. Current-density/voltage characteristics obtained with a nanocrystalline TiO₂ film supported on FTO conducting glass and derivatized with monolayer of the sensitizers; —: LI-1; - - - -: LI-2.

ters are list in Table 2, in comparison with those of the standard ruthenium dye N719 fabricated and measured under the same conditions. The DSSC based on LI-1 shows better

Table 2. Performance parameters of DSSCs vonstructed by using LI-1 and LI-2.

	$J_{sc}^{[a]}$ [mA cm ⁻²]	$V_{oc}^{[b]}$ [V]	$FF^{[c]}$	$\eta^{[d]}$ [%]	$\tau_n^{[e]}$ [ms]
LI-1	16.34	0.72	0.61	7.21	4.01
LI-2	10.50	0.71	0.62	4.62	2.79
N719	16.65	0.75	0.63	7.88	7.62

[a] J_{sc} = short circuit photocurrent density. [b] V_{oc} = open circuit voltage. [c] FF = fill factor. [d] η = overall light to electricity conversion efficiency. [e] The lifetime (τ_n) of injected electrons in the films can be drawn by the positions of the low-frequency peak in Figure 4 (bottom) through the expression $\tau_n = 1/(2\pi f)$, in which f is the frequency of the superimposed ac voltage.^[16]

comprehensive properties with an open circuit voltage of 0.72 V, a short circuit photocurrent density of 16.34 mA cm⁻², and a fill factor of 0.61, corresponding to an overall light to electricity conversion efficiency of 7.21 %, which is 91 % of the standard cell from N719 (7.88 %). The higher efficiency benefits from the highest short-circuit photocurrent density, which is about 6.0 higher than that of LI-2. Also, the three-dimensional structure of the TPA moiety linked to the nitrogen atom of pyrrole ring, in contrast to the more planar Cz one, will surely contribute to the suppression of the aggregation of the LI-1 on the surface of TiO₂ to a larger degree, resulting in the better power conversion efficiency directly.

This can be explained from the electrochemical impedance spectroscopy (EIS) of the DSSCs. Generally, three characteristic frequency peaks can be obtained from EIS spectra (Bode phase plot) when DSSCs are controlled under open-circuit conditions under light illumination. The low-frequency peak (in the mHz range) is attributed mainly to the Nernst diffusion of I₃⁻ within the electrolyte. The middle-frequency peak (in the 10–100 Hz region) is related to the transport process of the injected electrons within TiO₂ porous films and the charge-transfer process of the injected electrons at the interfaces between TiO₂ and the electrolyte/dye coating. The high-frequency peak (in the kHz range) is ascribed to the charge-transfer process at the interfaces between the redox couple and the platinized counter electrode. Figure 4 (bottom) shows the Bode phase plots of EIS spectra for the DSSCs made with TiO₂ electrodes dipped with different sensitizers. In our system, the low- and high-frequency peaks are similar, as the DSSCs are under the same conditions except for the sensitizer is different. However, distinct changes appeared in the middle frequency depending on the various sensitizers. The interfacial charge-transfer resistance (R_{CT}), calculated from the middle-frequency of EIS based on various sensitizers, is 10.95 Ω and 15.54 Ω . As can be seen, the sensitizer LI-1 shows the lower R_{CT} value, which indicated that the catalytic I₃⁻ reduction and electron transfer in DSSCs based on sensitizer LI-1 are the most efficient.

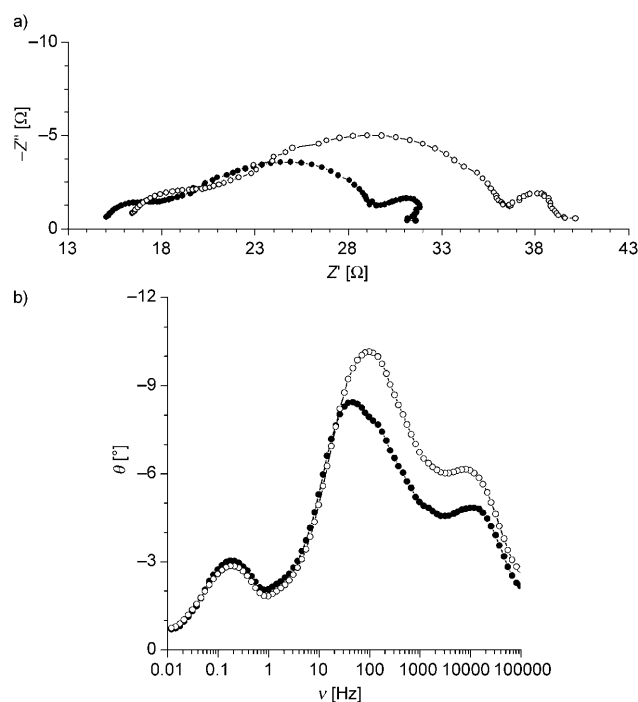


Figure 4. Electrochemical impedance spectroscopy (EIS) for DSSCs based on the sensitizers. Top: Nyquist plots. Bottom: Bode phase plots. ●: LI-1, ○: LI-2.

To increase the efficiency of DSSCs, an increase of the electron lifetime is essential. The photoelectrons that possess longer lifetimes have the more chance of entering the external circuit and contributing to the photoelectric conversion efficiency.^[17] As can be seen from Table 2, the injected electrons have the longer lifetime (4.01 ms) from the device based on the sensitizer LI-1, which is found to be in parallel with the trend of the cell efficiencies.

In conclusion, two novel metal-free organic dyes (namely, LI-1 and LI-2) with simple structures, were conveniently prepared and characterized. Thanks to the special electronic properties of pyrrole moieties and the introduction of the non-coplanar aromatic rings through single bond, a solar-cell device based on the sensitizer LI-1 yields an overall conversion efficiency of 7.21 % (91 % of the standard cell from N719, 7.88 %). The syntheses of more pyrrole-containing organic dyes are still in progress in our laboratory.

Experimental Section

The experimental details for the synthesis and characterization of the dyes LI-1 and LI-2 are given in the Supporting Information.

Acknowledgements

We are grateful to the National Science Foundation of China (no. 20674059, 20871096 and 20772094), the Program for NCET, the National Fundamental Key Research Program and Hubei Province for financial support.

Keywords: density functional calculations • dye/pigments • electrochemistry • pyrroles • solar cells

- [1] a) B. O'Regan, M. Grätzel, *Nature* **1991**, 353, 737–740; b) A. Hagfeldt, M. Grätzel, *Chem. Rev.* **1995**, 95, 49–68; c) M. Grätzel, *Nature* **2001**, 414, 338–344.
- [2] a) M. K. Nazeeruddin, P. Pechy, T. Renouard, S. M. Zakeeruddin, R. Humphry-Baker, P. Comte, P. Liska, L. Cevey, E. Costa, V. Shklover, L. Spiccia, G. B. Deacon, C. A. Bignozzi, M. Grätzel, *J. Am. Chem. Soc.* **2001**, 123, 1613–1624; b) M. K. Nazeeruddin, F. De Angelis, S. Fantacci, A. Selloni, G. Viscardi, P. Liska, S. Ito, T. Bessho, M. Grätzel, *J. Am. Chem. Soc.* **2005**, 127, 16835–16847; c) M. Grätzel, *J. Photochem. Photobiol. A* **2004**, 164, 3–14.
- [3] a) S. Ito, S. M. Zakeeruddin, R. Humphry-Baker, P. Liska, R. Charvet, P. Comte, M. K. Nazeeruddin, P. Pechy, M. Takata, H. Miura, S. Uchida, M. Grätzel, *Adv. Mater.* **2006**, 18, 1202–1205; b) T. Horiuchi, H. Miura, K. Sumioka, S. Uchida, *J. Am. Chem. Soc.* **2004**, 126, 12218–12219; c) Z. S. Wang, F. Y. Li, C. H. Huang, *J. Phys. Chem. B* **2001**, 105, 9210–9217; d) K. Hara, T. Sato, R. Katoh, A. Furube, Y. Ohga, A. Shinpo, S. Suga, K. Sayama, H. Sugihara, H. Arakawa, *J. Phys. Chem. B* **2003**, 107, 597–606.
- [4] S. Kim, J. K. Lee, S. O. Kang, J. Ko, J. H. Yum, S. Fantacci, F. De Angelis, D. D. Censo, M. K. Nazeeruddin, M. Grätzel, *J. Am. Chem. Soc.* **2006**, 128, 16701–16707.
- [5] a) D. P. Hagberg, T. Edvinsson, T. Marinado, G. Boschloo, A. Hagfeldt, L. Sun, *Chem. Commun.* **2006**, 2245–2247; b) J. T. Lin, P. C. Chen, Y. S. Yen, Y. C. Hsu, H. H. Chou, M. C. P. Yeh, *Org. Lett.* **2009**, 11, 97–100.
- [6] Y. S. Yen, Y. C. Hsu, J. T. Lin, C. W. Chang, C. P. Hsu, D. J. Yin, *J. Phys. Chem. C* **2008**, 112, 12557–12567.
- [7] a) J. Nakazaki, I. Chung, M. M. Matsushita, T. Sugawara, R. Watanabe, A. Izuoka, Y. Kawada, *J. Mater. Chem.* **2003**, 13, 1011–1022; b) B. K. Banik, S. Samajdar, I. Banik, *J. Org. Chem.* **2004**, 69, 213–216.
- [8] a) N. Basari, E. Marini, M. I. Kulyk, *J. Org. Chem.* **2003**, 68, 7524–7527; b) H. Y. Chen, Y. Chi, C. S. Liu, J. K. Yu, Y. M. Cheng, K. S. Chem, P. T. Chou, S. M. Peng, G. H. Lee, A. J. Carty, S. J. Yeh, C. T. Chen, *Adv. Funct. Mater.* **2005**, 15, 567–574.
- [9] a) Q. Q. Li, C. G. Lu, J. Zhu, E. Q. Fu, C. Zhong, S. Y. Li, Y. P. Cui, J. G. Qin, Z. Li, *J. Phys. Chem. B* **2008**, 112, 4545–4551; b) X. H. Ma, R. Liang, F. Yang, Z. H. Zhao, A. X. Zhang, N. H. Song, Q. F. Zhou, J. P. Zhang, *J. Mater. Chem.* **2008**, 18, 1756–1764; c) O. P. Kwon, M. Jazbinsek, H. Yun, J. I. Seo, E. M. Kim, Y. S. Lee, P. Günter, *Cryst. Growth Des.* **2008**, 8, 4021–4025; d) M. M. M. Raposo, A. M. R. C. Sousa, G. Kirsch, P. Cardoso, M. Belsley, E. de Matos Gomes, A. M. C. Fonseca, *Org. Lett.* **2006**, 8, 3681–3684.
- [10] a) S. J. Zheng, L. Beverina, S. Barlow, E. Zojer, J. Fu, L. A. Padilha, C. Fink, O. Kwon, Y. P. Yi, Z. G. Shuai, E. W. V. Stryland, D. J. Hagan, J. L. Brédas, S. R. Marder, *Chem. Commun.* **2007**, 1372–1374; b) L. Beverina, J. Fu, A. Leclercq, E. Zojer, P. Pacher, S. Barlow, E. W. Van Stryland, D. J. Hagan, J. L. Brédas, S. R. Marder, *J. Am. Chem. Soc.* **2005**, 127, 7282–7283.
- [11] a) D. P. Hagberg, J. H. Yum, H. Lee, F. De Angelis, T. Marinado, K. M. Karlsson, R. H. Baker, L. Sun, A. Hagfeldt, M. Grätzel, M. K. Nazeeruddin, *J. Am. Chem. Soc.* **2008**, 130, 6259–6266; b) D. Liu, R. W. Fessenden, G. L. Hug, P. V. Kamat, *J. Phys. Chem. B* **1997**, 101, 2583–2590; c) B. Burfeindt, T. Hannappel, W. Storck, F. Willig, *J. Phys. Chem.* **1996**, 100, 16463–16465; d) K. Sayama, S. Tsukagoshi, K. Hara, Y. Ohga, A. Shinpo, Y. Abe, S. Suga, H. Arakawa, *J. Phys. Chem. B* **2002**, 106, 1363–1371; e) C. Kim, H. Choi, S. Kim, C. Baik, K. Song, M. S. Kang, S. O. Kang, J. Ko, *J. Org. Chem.* **2008**, 73, 7072–7079.
- [12] a) Q. Zeng, Z. Li, Y. Dong, C. Di, A. Qin, Y. Hong, Z. Zhu, C. K. W. Jim, G. Yu, Q. Li, Z. Li, Y. Liu, J. Qin, B. Z. Tang, *Chem. Commun.* **2007**, 70–72; b) Q. Q. Li, Z. Li, S. S. Yu, J. G. Qin, *J. Phys. Org. Chem.* **2009**, 22, 241–246; c) S. Dong, Z. Li, J. Qin, *J. Phys. Chem. B* **2009**, 113, 434–441.
- [13] Z. Delen, P. M. Lahti, *J. Org. Chem.* **2006**, 71, 9341–9347.
- [14] a) K. R. J. Thomas, Y. C. Hsu, J. T. Lin, K. M. Lee, K. C. Ho, C. H. Lai, Y. M. Cheng, P. T. Chou, *Chem. Mater.* **2008**, 20, 1830–1840; b) H. N. Tian, X. C. Yang, R. K. Chen, R. Zhang, A. Hagfeldt, L. C. Sun, *J. Phys. Chem. C* **2008**, 112, 11023–11033; c) K. Hara, Z. S. Wang, T. Sato, A. Furube, R. Katoh, H. Sugihara, Y. Dan-oh, C. Kasada; d) R. K. Chen, X. C. Yang, H. Tian, X. Wang, A. Hagfeldt, L. C. Sun, *Chem. Mater.* **2007**, 19, 4007–4015; e) Gaussian 03, Revision E.1, M. J. Frisch, G. W. Trucks, H. B. Schlegel, G. E. Scuseria, M. A. Robb, J. R. Cheeseman, J. A. Montgomery, Jr., T. Vreven, K. N. Kudin, J. C. Burant, J. M. Millam, S. S. Iyengar, J. Tomasi, V. Barone, B. Mennucci, M. Cossi, G. Scalmani, N. Rega, G. A. Petersson, H. Nakatsuji, M. Hada, M. Ehara, K. Toyota, R. Fukuda, J. Hasegawa, M. Ishida, T. Nakajima, Y. Honda, O. Kitao, H. Nakai, M. Klene, X. Li, J. E. Knox, H. P. Hratchian, J. B. Cross, C. Adamo, J. Jaramillo, R. Gomperts, R. E. Stratmann, O. Yazyev, A. J. Austin, R. Cammi, C. Pomelli, J. W. Ochterski, P. Y. Ayala, K. Morokuma, G. A. Voth, P. Salvador, J. J. Dannenberg, V. G. Zakrzewski, S. Dapprich, A. D. Daniels, M. C. Strain, O. Farkas, D. K. Malick, A. D. Rabuck, K. Raghavachari, J. B. Foresman, J. V. Ortiz, Q. Cui, A. G. Baboul, S. Clifford, J. Cioslowski, B. B. Stefanov, G. Liu, A. Liashenko, P. Piskorz, I. Komaromi, R. L. Martin, D. J. Fox, T. Keith, M. A. Al-Laham, C. Y. Peng, A. Nanayakkara, M. Challacombe, P. M. W. Gill, B. Johnson, W. Chen, M. W. Wong, C. Gonzalez, J. A. Pople, Gaussian, Inc., Pittsburgh PA, **2003**.
- [15] D. P. Hagberg, T. Edvinsson, T. Marinado, G. Boschloo, A. Hagfeldt, L. Sun, *Chem. Commun.* **2006**, 2245–2247.
- [16] R. Kern, R. Sastrawan, J. Ferber, R. Stangl, J. Luther, *Electrochim. Acta* **2002**, 47, 4213–4225.
- [17] a) S. Soedergren, A. Hagfeldt, J. Olsson, S. E. Lindquist, *J. Phys. Chem.* **1994**, 98, 5552–5556; b) N. Koumura, Z. S. Wang, S. Mori, M. Miyashita, E. Suzuki, K. Hara, *J. Am. Chem. Soc.* **2006**, 128, 14256–14257.

Received: April 30, 2009
Published online: August 15, 2009